

1
2
3 Title: ~~Long-term sulphide mitigation through molybdate at shrimp pond bottoms~~ **Molybdate**
4 **delays sulphide formation in the sediment and transfer to the bulk liquid in a model**
5 **shrimp pond**

6
7 Running title: Long-term inhibition of sulphate reduction through molybdate

8
9 **Funda Torun¹, Barbara Hostins², Peter De Schryver², Nico Boon^{1,3}, Jo De Vrieze^{1,3}✉**

10
11 ¹ Center for Microbial Ecology and Technology (CMET), Ghent University, Coupure Links
12 653, Ghent 9000, Belgium

13 ² INVE Technologies NV, Hoogveld 93, Dendermonde, Belgium

14 ³ Centre for Advanced Process Technology for Urban Resource recovery (CAPTURE), P.O.
15 Frieda Saeystraat 1, B-9000 Gent, Belgium

16
17
18
19
20
21 ✉ Correspondence to: Jo De Vrieze, Ghent University; Faculty of Bioscience Engineering;
22 Center for Microbial Ecology and Technology (CMET); Coupure Links 653; B-9000 Gent,
23 Belgium; phone: +32 (0)9 264 59 76; E-mail: Jo.DeVrieze@UGent.be; Webpage:
24 www.cmet.ugent.be.

26 **Abstract**

27 Shrimp are commonly cultured in earthen aquaculture ponds where organic-rich uneaten feed
28 and faeces accumulate on and in the sediment to form anaerobic zones. Since the pond water is
29 rich in sulphate, these anaerobic conditions eventually lead to the production of sulphide.
30 Sulphides are toxic and even lethal to the shrimp that live on the pond sediment, but
31 physicochemical and microbial reactions that occur during the accumulation of organic waste
32 and the subsequent formation of sulphide in shrimp pond sediments remain unclear. Molybdate
33 treatment is a promising strategy to inhibit sulphate reduction, thus, preventing sulphide
34 accumulation. We used an experimental shrimp pond model to simulate the organic waste
35 accumulation and sulphide formation in a long-term experiment (61 days) during the final 61
36 days of a full shrimp growth cycle. Sodium molybdate (5 and 25 mg/L $\text{Na}_2\text{MoO}_4 \cdot 2\text{H}_2\text{O}$) was
37 applied as a preventive strategy to control sulphide production before oxygen depletion.
38 Molybdate addition partially mitigated H_2S production in the sediment, and delayed its transfer
39 to the bulk liquid by pushing the higher sulphide concentration zone towards deeper sediment
40 layers. Molybdate treatment at 25 mg/L significantly impacted the overall microbial community
41 composition and treated samples (5 and 25 mg/L molybdate) had about 50% higher relative
42 abundance of sulphate reducing bacteria than the control (no molybdate) treatment. In
43 conclusion, molybdate worked has the potential to work as long-term mitigation strategy
44 against sulphide accumulation in the sediment during shrimp growth by directly steering the
45 microbial community in a shrimp pond system.

46

47 **Keywords:** Aquaculture, molybdate, shrimp growth, sulphate reduction, sulphide toxicity

48

49 **1. Introduction**

50 The properties of pond bottom soil (sediment) and physicochemical and microbial interactions
51 on and in the sediment are crucial for the well-being and growth of the shrimp in aquaculture
52 ponds (Avnimelech and Ritvo, 2003; Burford et al., 1998). Sediments contain indigenous
53 nutrients and organic matter, derived directly from the environment, but also from uneaten and
54 digested feed of the numerous shrimp that dwell on the pond bottom, especially during semi-
55 intensive and intensive stocking (50-300 shrimp/m³) (Avnimelech and Ritvo, 2003). This pond
56 bottom layer, *i.e.*, the interphase between the water and sediment, is an area that is densely
57 populated by microorganisms consuming the available organic matter. Due to the organic-rich
58 conditions on the pond bottom in combination with the typical temperatures of 25-30 °C in
59 shrimp ponds, the oxygen consumption by these microorganisms can cause a rapid drop in
60 dissolved oxygen in the sediment (Baxa et al., 2021; Dien et al., 2019). When oxygen
61 consumption exceeds the rate of oxygen transfer from the pond water phase to the sediment,
62 eventually sediment oxygen is depleted, and anaerobic conditions arise. Due to high sulphate
63 concentrations in the pond water, low redox conditions in the pond lead to production of
64 hydrogen sulphide (H₂S) from metabolic activity of sulphate reducing bacteria (SRB)
65 (Avnimelech and Ritvo, 2003; Boyd, 1998). The H₂S formed creates a bad odour and black
66 colour in the sediment, and is also toxic to the shrimp that dwell at the pond bottom. Sulphide
67 toxicity to shrimp depends on both the H₂S concentration and pH (Thulasi et al., 2020;
68 Vismann, 1996), with lethal concentrations to kill 50% of the population (LC50) values ranging
69 between 0.0087 and 0.033 mg/L H₂S, depending on shrimp species and growth phase of the
70 shrimp (Chen, 1985; US-EPA, 2011). Exposure to sub-lethal concentrations of H₂S lowers
71 shrimp resistance to diseases and causes tissue corrosion (Suo et al., 2017). Overall, H₂S is
72 often the main cause for mortality or abnormal behaviour of shrimp, and may strongly impact
73 shrimp harvest (Panakorn, 2016).

74 Sulphide accumulation in shrimp ponds conventionally relies on labour-intensive, time-
75 intensive and costly approaches, such as mechanical removal of reduced sediment or change of
76 culture water. An alternative approach is nitrate amendment, which has been shown to remove
77 the H₂S produced (Torun et al., 2020). However, as also demonstrated for sodium percarbonate,
78 the effect of nitrate towards sulphide removal was only transient, because when nitrate was
79 depleted, the H₂S production recovered (Schwermer et al., 2010; Torun et al., 2022; Torun et
80 al., 2020), requiring higher amounts of nitrate addition to compete with sulphate reduction.
81 Repeated and/or increased addition of nitrate is unwanted, because this may result in
82 cyanobacteria and algal blooms or the release of toxic metabolites, *e.g.*, nitrite or nitrous oxide.
83 A more targeted, preventive approach that achieves direct inhibition of the SRB, thus,
84 preventing sulphide production, is the application of molybdate (MoO₄). Because of its
85 stereochemical similarity to sulphate, molybdate inhibits the adenosine triphosphate
86 sulfurylase, which is the first enzyme in the sulphate reduction pathway (Peck, 1959; Stoeva
87 and Coates, 2019). Successful inhibition of sulphate reduction through the addition of
88 molybdate has been observed in studies on eutrophic lake sediments (Smith and Klug, 1981),
89 anaerobic digestion (Isa and Anderson, 2005; Ranade et al., 1999), and oil production systems
90 (Jesus et al., 2015; Kögler et al., 2021). Hence, its application in aquaculture systems also
91 warrants possibilities towards preventing H₂S formation in pond sediments. This was
92 demonstrated in a short-term experiment with a shrimp pond model in which molybdate
93 outperformed nitrate and sodium percarbonate in controlling H₂S formation, because of its
94 specificity and preventive mode of action (Torun et al., 2022). **The applicability of molybdate**
95 **as a remediation strategy towards sulphide formation in aquaculture, however, strongly depends**
96 **on its ~~long-term~~ lasting effect during a 90-days shrimp growth cycle.**
97 **The objective of this study was to determine the ~~long-term~~ duration and magnitude of the**
98 **effect of molybdate towards H₂S mitigation in response to the gradual accumulation of organic**

99 waste during a full shrimp growth cycle. A shift in the microbial community towards different
100 processes than sulphate reduction, in response to molybdate, could be beneficial to control
101 sulphide accumulation at the shrimp pond bottom. Because the accumulation of organic waste
102 was limited during the first 30 days of the shrimp growth cycle, *i.e.*, no O₂ depletion or H₂S
103 accumulation (Torun et al., 2023), only the final 61 days were considered in a lab-scale shrimp
104 pond bottom model.

105 **2. Material and methods**

106 2.1. Sampling and storage

107 2.1.1. Sediment sampling

108 Sandy clay and organic-rich sediments were obtained from the Ijzermonding Nature Reserve
109 (Nieuwpoort, Belgium) from a creek (51°8'45" N/2°44'38"E) that was regularly water-logged
110 with tidal movement. Sampling were taken by scooping the top 5-10 cm of the sediment into a
111 closed plastic container in which they were transported to the laboratory. The pH, conductivity,
112 total solids (TS) and volatile solids (VS) of the fresh sediment were analysed directly upon
113 arrival in the laboratory. A sample for sulphate and molybdate analysis was stored at 4°C until
114 analysis, and a sample for DNA extraction was stored at -20°C.

115

116 2.1.2. Feed and faeces collection and storage

117 Fresh shrimp faeces were collected from the flush outlet of shrimp tanks in which whiteleg
118 shrimp (*Litopenaeus vannamei*) at post-larvae stage were fed with CreveTec Grower 2
119 (CreveTec, Ternat, Belgium) at the Aquaculture and *Artemia* Reference Center (ARC), Faculty
120 of Bioscience and Engineering, Ghent University, Belgium. The faeces were stored at 4°C until
121 use to avoid organic matter degradation during storage. The pH and conductivity of the faeces
122 were measured directly after collection. A sample for DNA extraction was stored at -20°C.

123

124 2.2. Experimental set-up and operation

125 A system mimicking organic matter accumulation in the shrimp ponds was designed and
126 constructed, as described earlier (Torun et al., 2022), using 250 mL size glass beakers (outer
127 diameter 70 mm) containing a 3.5 cm sediment layer and 5 cm overlaying artificial seawater
128 (Instant Ocean, Aquarium Systems, Mentor, OH, USA). The salinity of the artificial seawater
129 was adjusted to 20 g/L, representing a common salinity in shrimp ponds (15-25 g/L), and

130 containing approximately 1.5 g/L sulphate. To avoid excessive water evaporation, the beakers
131 were put in a transparent plastic box with a non-airtight lid in a temperature-controlled room at
132 $28 \pm 1^\circ\text{C}$ without active aeration. **No artificial or natural light was foreseen to avoid the**
133 **growth of microalgae and keep a focused approach towards sulphide formation and**
134 **oxygen depletion.**

135 The experiment was started with an initial cumulative waste of 30 days of shrimp culture (DOC
136 30) in the form of feed (CreveTec Grower 2 shrimp feed) and faeces, which was considered
137 day zero of the experiment. The cumulative waste for shrimp culture was calculated based on
138 the 0.003848 m^2 bottom surface area of the beakers using commercial daily shrimp feeding
139 tables (Table S1). Feed and faeces were added based on semi-intensive stocking of 50
140 shrimp/ m^2 . About 25% of input feed was assumed to be accumulating in the pond bottom, with
141 15% considered digested feed (faeces), and 10% as uneaten feed. After adding the initial waste
142 of DOC 30, the respective amount of shrimp feed and faeces, based on daily uneaten feed and
143 faeces, were supplemented every 2-3 days (Table S2). The amounts of supplemented feed and
144 faeces were increased every 15 days to adapt to the growth of the shrimp.

145 **Two different concentrations of 5 (M5) and 25 (M25) mg/L of sodium molybdate**
146 **($\text{Na}_2\text{Mo}_4 \cdot 2\text{H}_2\text{O}$, Sigma Aldrich, St. Louis, Mo., US), were compared with a control treatment**
147 **(no molybdate addition) for a long-term experiment of the last 61 days of a shrimp growth**
148 **cycle.** Molybdate was supplemented in a single dose on day 0 of the experiment. Each treatment
149 was carried out in 6 biological replicates. Measurements of dissolved oxygen (DO), H_2S and
150 pH in the bulk liquid were performed every 2-3 days. These measurements were taken from the
151 water column, about 1 cm above the sediment-water interface, since H_2S in the bulk liquid is
152 the major concern for the shrimp that dwell on the pond bottom. Apart from bulk liquid
153 measurements, microscale gradient depth profiles of DO, H_2S and pH at the water-sediment
154 interface and throughout the sediment were measured, using a microelectrode, on day 16, 30,

155 44 and 61 from three replicates of each treatment. After each depth profiling measurement (day
156 16, 30, 44), one replicate from each treatment was sacrificed for the measurement of molybdate
157 and sulphate concentrations in the bulk liquid. From these sacrificial beakers, sediment samples
158 were taken, and stored at -20°C for microbial community analysis. At the end of the experiment
159 (day 61), all remaining replicates (3 replicates) were sampled for sediment and liquid samples.
160 Sediment samples were taken from the upper 1 cm of the sediment layer after carefully
161 decanting the liquid part. The liquid samples were filtered over a 0.20 µm Chromafil® Xtra filter
162 (Macherey-Nagel, PA, USA), and stored at 4 °C, prior to analysis of sulphate and molybdate
163 concentrations. During each liquid sampling, the degree of water evaporation was determined
164 by recording the water depth. The molybdate and sulphate measurements were corrected with
165 the evaporation factor.

166

167 2.3. Microelectrode measurements

168 Microscale depth profiles of O₂, pH and H₂S were recorded using commercial microelectrodes
169 (Unisense A.S. Denmark, tip sizes pH: 200 µm, H₂S: 100 µm, O₂: 100 µm), operated with a
170 motorized micromanipulator (Unisense A. S., Denmark). Microscale measurements were
171 always performed before other samples were taken and before adding fresh waste to avoid
172 disturbance of the water column and sediment. The oxygen profiles were measured at 200 µm
173 resolution. The pH and H₂S were simultaneously recorded with the same resolution at 200 µm
174 in the water-sediment interphase, and at lower resolution deeper in the sediment. The sensors
175 were calibrated following standard calibration procedures, as described earlier (Malkin et al.,
176 2014). The H₂S was calibrated with a 3-5 point standard curve using an acidified Na₂S standard
177 solution (pH 3.5-4.0). The O₂ sensor was calibrated with a 2 point standard curve, using 100%
178 in air bubbled seawater for the DO at saturation at 28°C and argon bubbled seawater for DO
179 zero. The pH sensor was calibrated with 2 point calibrations using commercial (Carl Roth

180 GmbH & Co.KG, Karlsruhe, Germany) pH buffer solutions (4, and 7). Total sulphide
181 concentrations were calculated as described earlier (Jeroschewski et al., 1996). For bulk liquid
182 measurements, the same electrodes were used manually to take the measurements from
183 approximately 1 cm above the sediment surface after ensuring that there was negligible variety
184 in the duplicate measurements of the water column parameters.

185

186 2.4. Analytical techniques

187 The TS and VS of the sediment were determined according to Standard Methods (Greenberg et
188 al., 1992). The pH of the overlaying water and sediment samples were measured with a pH
189 meter (Metrohm, Herisau, Switzerland), which was calibrated using pH buffer solutions at pH
190 4 and 7. The sulphate concentrations were measured through ion chromatography (930
191 Compact IC Flex, Metrohm, Herisau, Switzerland), equipped with a Metrosep A supp 5–
192 150/4.0 anion column with conductivity detector, after diluting the samples 1:50 using ultra-
193 pure water (Milli-Q, Millipore Corporation, Burlington, MA, USA). The detection range was
194 0.05 to 200 mg ion/L. Molybdate was measured using a commercial kit (Hach, Model Mo-2,
195 USA), based on the colorimetric determination of molybdenum using mercaptoacetic acid (Will
196 and Yoe, 1953). Standard solutions of 0, 5, 10, 25, and 50 mg/L $\text{Na}_2\text{MoO}_4 \cdot 2\text{H}_2\text{O}$ were prepared
197 to determine the standard curve at 425 nm using a UV-Vis Spectrophotometer (WPA Lightwave
198 II, Thermofisher, USA).

199

200 2.5. Microbial community analysis

201 2.5.1. Amplicon sequencing

202 To analyse the changes in the bacterial community and SRB relative abundance, samples were
203 taken from the upper 1 cm of the sediment from each sacrificial beakers in 3 replicates and
204 frozen at -20 °C. The DNA was extracted directly from the frozen samples using a commercial

205 kit (DNeasy Power Soil Pro Kit, QIAGEN, Hilden, Germany), following the instructions of the
206 manufacturer. The quality of the DNA extracts was evaluated through agarose gel
207 electrophoresis and PCR analysis with the universal bacterial primers 341F (5'-
208 CCTACGGGNGGCWGCAG) and 785Rmod (5'-GACTACHVGGGTATCTAAKCC) that
209 target the V3-V4 region of the 16S rRNA gene (Klindworth et al., 2013), following a PCR
210 protocol as described earlier (Boon et al., 2002). The samples were sent to LGC Genomics
211 GmbH (Berlin, Germany) for Illumina amplicon sequencing of the V3-V4 region of the 16S
212 rRNA gene of the bacterial community on the MiSeq platform with V3 chemistry. The
213 amplicon sequencing protocol and data processing are described in detail in the SI (S3).

214

215 2.5.2. Flow cytometry analysis

216 Absolute microbial cell counts in the sediment samples were determined using flow cytometry
217 (FCM). Prior to FCM analysis, sediment samples were defrosted, acclimated to room
218 temperature and diluted tenfold in sterile, 0.22 µm-filtered Instant Ocean® solution. To separate
219 the cells from sediment particles, samples were initially sonicated (Q700 Sonicator, Qsonica,
220 Newtown, CT, USA) for 3 minutes, followed by 3 minutes centrifugation at 500 g. The resulting
221 supernatant of the samples was stained with 1 vol% SYBR® Green I (SG, 100x concentrate in
222 0.22 µm-filtered DMSO, Invitrogen), and incubated in the dark at 37°C for 20 min. Immediately
223 after incubation, samples were analysed using a BD Accuri C6 Plus cytometer (BD Biosciences,
224 Erembodegem, Belgium), equipped with four fluorescence detectors (533/30 nm, 585/40 nm,
225 > 670 528 nm and 675/25 nm), two scatter detectors and a 20-mW 488-nm laser. Samples were
226 analysed in fixed volume mode (30 µL). The flow cytometer was operated with Milli-Q water
227 (MerckMillipore, Belgium) as sheath fluid, and instrument performance was verified daily
228 using CS&T RUO Beads (BD Biosciences, Erembodegem, Belgium).

229

230 2.6. Statistical analysis

231 A table containing the relative abundances of the different OTUs (operational taxonomic units),
232 and their taxonomic assignment was created following amplicon data processing
233 (Supplementary Information File 2). All statistical analysis were carried out in R Studio version
234 4.03 (<http://www.r-project.org>) (R Development Core Team, 2013). A repeated measures
235 analysis of variance (ANOVA, *aov* function) was used to validate that the biological replicates
236 showed no significant ($P < 0.05$) differences in bacterial community composition. Next,
237 absolute singletons were removed, and the different samples were rescaled *via* the “common-
238 scale” approach (McMurdie and Holmes, 2014) through which the proportions of all OTUs
239 were taken, multiplied with the minimum sample size, and rounded to the nearest integer.
240 Sampling depth of each sample was evaluated through rarefaction curves (Figure S1) (Hurlbert,
241 1971; Sanders, 1968). The packages *vegan* (Oksanen et al., 2016) and *phyloseq* (McMurdie and
242 Holmes, 2013) were used for microbial community analysis. A heatmap was created at the
243 phylum and family level (1% cut-off) with the *pheatmap* function (*pheatmap* package), and
244 biological replicates were collated according to the method described earlier (Connelly et al.,
245 2017). The non-metric multidimensional scaling (NMDS) plots were constructed using the
246 Bray-Curtis (Bray and Curtis, 1957) distance measures. Significant differences between
247 treatments and timepoints were identified using pairwise permutational ANOVA
248 (PERMANOVA) analysis (9999 permutations) with Bonferroni correction, using the *adonis*
249 function (*vegan*).

250 **3. Results**

251 3.1. Impact of molybdate on oxygen depletion and sulphide production

252 3.1.1. Bulk liquid concentrations

253 The DO measurements in the bulk liquid showed that oxygen was completely depleted for the
254 first time on day 7 for all treatments (Figure 1a). In the following days, there was a fluctuation
255 in oxygen concentrations, *i.e.*, between 0 and 150 μM , for all treatments, with a regular oxygen
256 re-introduction in the bulk between day 7 to 35, keeping in mind that no active aeration was
257 applied. After day 35 of the experiment, a full oxygen depletion was observed for all treatments
258 with only limited oxygen re-introduction, resulting in oxygen concentrations only up to 50 μM .
259 For the entire experimental period, the DO concentration in the bulk did not show clear
260 difference between the different treatments, and also pH remained similar in the different
261 treatments (Figure S2).

262 No clear H_2S production was observed, *i.e.*, H_2S concentrations did not exceed 10 μM , in the
263 bulk liquid until day 35 of the experiment, coinciding with the time when oxygen depletion for
264 all incubations was recorded (Figure 1b). On day 35, a H_2S concentration of 64 ± 7 , 53 ± 11 ,
265 and 39 ± 3 μM was recorded in the bulk liquid for the control, M5, and M25 treatments,
266 respectively. This corresponded with a total bulk sulphide concentration that was 22 ± 1 % and
267 46 ± 1 % lower than the control for M5 and M25, respectively (Figure S3). Hence, there was
268 markedly lower H_2S production in the molybdate treatments compared to the control treatment,
269 especially in the M25 treatment. Also on day 56 of the experiment, H_2S concentration in the
270 bulk was clearly higher in the control treatment ($16 + 5$ μM) compared to the M5 ($7 + 6$ μM)
271 and M25 ($5 + 5$ μM) treatments.

272 Residual molybdate measurements indicated that about 53 ± 1 % of the dosed molybdate
273 disappeared from the bulk liquid for M25 at the end of the experiment, while this ranged
274 between 5-15% for M5. (Table 1). Hence, in both molybdate treatments, residual molybdate

275 remained present. Residual sulphate concentration in the bulk gradually decreased throughout
276 the experiment, yet, no clear differences could be observed between the treatments (Table 2).

277

278 3.1.2. Sediment profiles

279 Microscale depth profiles of the DO in the sediment on day 16 revealed a 12 ± 4 % higher
280 concentration of oxygen in the M25 compared to the control treatment at the water-sediment
281 interface (Figure 2). Oxygen diffusion into the first 2 mm of the upper sediment layer was
282 observed for all treatments, with negligible differences between the treatments. On day 30, the
283 DO depth profile showed no apparent difference between the different treatments On day 44
284 and 61, no more oxygen was detected in the bulk liquid or sediment.

285 Microscale depth profiles of H₂S in the sediment were recorded on day 16, 44 and 61, while
286 day 30 gradient measurements of H₂S could not be obtained, due to technical problems with
287 the microelectrode (Figure 3). On day 16, although no H₂S could be observed in the bulk liquid,
288 H₂S gradient measurements showed a minor H₂S production in the control reaching a
289 concentration up to 5.8 ± 0.1 μ M at the sediment depth of 3.6 mm, while for the M5 and M25
290 treatments, no H₂S production was observed. On day 44, the control treated showed a maximum
291 H₂S concentration of 66.6 ± 20.5 μ M in the sediment deeper layers (sediment depth of 6.0 mm).
292 The M5 and M25 treatments showed a maximum H₂S concentration of only 22.7 ± 4.2 μ M and
293 29.3 ± 26.8 μ M H₂S, respectively, both at 7.2 mm sediment depth, being 69 ± 11 and 60 ± 39
294 % lower than the maximum value in the control treatment, respectively. On day 61, the H₂S
295 concentration in the sediment was more similar between the different treatments, in contrast to
296 day 16 and 44. The M5 and M25 treatments showed a 17 ± 9 % and 26 ± 15 % lower maximum
297 H₂S concentration compared with the control, respectively. The H₂S production zone appeared
298 to be pushed to deeper sediment layers in the M5 and M25 treatments both for day 44 and 61
299 measurements, compared to the control. Total S microscale depth profiles showed a similar

300 pattern as the H₂S profiles (Figure S4), with the M5 and M25 treatments showing a markedly
301 lower total S concentration in the sediment in comparison with the control treatment. The pH
302 microscale depth profiles were similar between the different treatments, with limited variation
303 in function of time (Figure S5).

304

305 3.2. Microbial community analysis

306 Amplicon sequencing of the bacterial community resulted in an average of $23,917 \pm 9,397$
307 reads, which represented $2,922 \pm 876$ OTUs per sample (including singletons). Removal of
308 absolute singletons and rescaling through the “common-scale” approach resulted in an average
309 of $6,031 \pm 282$ reads and 681 ± 171 OTUs per sample. Repeated measures ANOVA revealed
310 no significant differences ($P < 0.0001$) between the biological replicates.

311 Shrimp faeces (day 0) were dominated by Bacteroidota (35.9 ± 7.8 %) and Fusobacteriota (35.1
312 ± 5.7 %) phyla, while the sediment used in the experiment was dominated by Actinobacteriota
313 (22.3 ± 8.8 %) and Proteobacteria (33.5 ± 1.6 %) phyla (Figure 4). The sediment samples (day
314 0) showed a relatively higher abundance of the phylum Desulfobacterota (4.2 ± 0.3 %), which
315 contains several sulphate reducers, than the shrimp faeces (0.2 ± 0.0 %) samples. Over time,
316 there was a clear shift in the bacterial communities, specifically for Proteobacteria, Bacteroidota
317 and Desulfobacterota relative abundances for all treatments. On day 16, the control, M5 and
318 M25 treatments showed markedly high relative abundances of Proteobacteria (29.3 ± 3.2 %, 27.2 ± 5.8 %, 30.7 ± 0.4 %, respectively). On day 30 and 44, the M5 and M25 treatment showed
319 an even further increase in the relative abundance of Proteobacteria (35.6 ± 6.7 % and $34.7 \pm$
320 6.2 % for day 30 and 34.2 ± 8.1 % and 38.0 ± 0.2 % for day 44, respectively), compared to the
321 control treatment (26.6 ± 4.0 % for day 30, 22.8 ± 3.1 % for day 44). This higher relative
322 abundance of Proteobacteria in the M5 and M25 treatments coincided with a more prominent
323 presence of the Rhodobacteraceae family (Figure S6) in the M5 (16.1 ± 4.5 %) and M25 (14.5
324

325 ± 7.2 %) treatments, compared to the control ($8.3 \pm 0.6\%$), on day 30 and later timepoints in
326 the experiment. The M5 (15.3 ± 3.2 %) and M25 (16.1 ± 4.1 %) treatment showed an overall
327 higher relative abundance of Flavobacteriaceae than the control treatment (12.3 ± 2.7 %). The
328 high relative abundance of Bacteroidota (Figure 4) likely originated from the addition of faeces,
329 and reached values of 27.9 ± 1.2 %, 27.9 ± 0.8 % and 20.5 ± 1.8 % on day 16 for the control,
330 M5 and M25 treatments, respectively. However, in time, the relative abundance of Bacteroidota
331 decreased in all treatments ($22.3 \pm 2.4\%$). There was no clear difference in Bacteroidota relative
332 abundance between the different treatments.

333 There was an apparent higher abundance of the Delsulfobacterota phylum, which contains
334 several sulphate reducers, in the M5 (15.3 ± 3.1 %) and M25 ($16.2 \pm 0.4\%$) treatments,
335 compared to the control treatment ($8.8 \pm 1.6\%$) for all samples on day 16, 30, 44 and 61. The
336 M25 treatment also showed a slightly higher abundance of this phyla compared to the M5
337 treatment. Family level analysis revealed that SRB species belonged to Desulfobulbaceae,
338 Desulfomonadaceae, Desulfolunaceae, Delsufovibrionaceae, Desulfosarcinaceae,
339 Delsulfobacteraceae and Desulfocapsaceae families (Figure S6). An absolute cell count
340 analysis of Delsulfobacterota phylum, by combining flow cytometry cell counts with amplicon
341 sequencing data, showed that all samples, including the samples treated with molybdate,
342 showed an increasing trend in time of absolute Delsulfobacterota cell counts. Molybdate treated
343 samples, especially M25, in general, showed even higher absolute cell counts for the
344 Desulfobacterota phylum compared to the control (Table 3).

345 The β -diversity analysis of the bacterial community, based on the Bray-Curtis distance measure,
346 revealed that the M25 treatment showed an overall significantly different bacterial community
347 composition than the control treatment ($P = 0.0003$) (Figure 5). However, none of the other
348 treatments significantly differed ($P > 0.05$), and there was a limited impact of molybdate
349 addition on the change of the bacterial community in function of time. The PERMANOVA

350 analysis showed that there was a significant change in overall bacterial community composition
351 between day 16 and 30 ($P = 0.0036$), day 30 and 44 ($P = 0.0174$) and day 44 and 61 ($P =$
352 0.0066). On day 61, at the end of the experiment, the bacterial community composition for all
353 treatments showed a clear divergence.

354 **4. Discussion**

355 This study showed that molybdate addition, prior to H₂S formation, has a good potential to
356 mitigate H₂S production in the sediment, and delay its transfer to the bulk liquid by pushing
357 sulphide production zone in deeper layers of the sediment. Bacterial community analysis
358 revealed a limited impact of molybdate addition on the change of the bacterial community in
359 function of time. Molybdate treated samples did show a higher absolute abundance of the
360 Desulfobacterota phylum compared to the control.

361

362 4.1. Molybdate effectively controls sulphide production and pushes higher sulphide
363 concentration zones towards deeper sediment layers

364 The typical shrimp pond water with a salinity of 1.5-2.5 % contains about 1500 mg/L sulphate
365 (Torun et al., 2020). This high availability of sulphate and organic-rich conditions in the pond
366 bottom make the shrimp pond environment susceptible to the production of sulphides when
367 anaerobic conditions arise, due to the depletion of oxygen. The most effective method for
368 avoiding anaerobic conditions is to keep dissolved oxygen levels sufficiently high for the entire
369 depth of the pond water. However, mechanical aeration is usually applied on the water surface
370 (e.g., paddlewheel aerators). Apart from being costly and energy-consuming, these aerators
371 come with a risk of causing erosion in the pond bottom soil, when the water current is too
372 strong. Erosion degrades embankments, makes the harvest more difficult, and damages benthic
373 plants and animal communities, including the shrimp (Boyd, 1998). **In a real pond system,**
374 **also the growth of microalgae could play a critical role, as they (1) enable in situ formation**
375 **of oxygen, and (2) by consuming CO₂, they could provoke an increase in pH, which could**
376 **reduce H₂S toxicity, but increase ammonia toxicity. They can even actively contribute to**
377 **an improved water quality (Huang et al., 2022). However, the direct involvement of**
378 **microalgae in our model system would strongly add to the complexity of sulphide**

379 **formation, because of their multi-level impact on the shrimp pond nutrient dynamics, so**
380 **we eliminated the possibility for photosynthetic growth from our model by not supplying**
381 **natural or artificial light.** Nitrate addition could serve as an alternative electron acceptor, in
382 competition with sulphate. However, nitrate can only temporarily control sulphide production,
383 and when nitrate is depleted, sulphide production recovers (Schwermer et al., 2010; Torun et
384 al., 2022; Torun et al., 2020). **These limitations substantiate the importance of a long-term**
385 **lasting strategy to mitigate sulphide production in shrimp pond aquaculture systems.**

386 In this study, 5 and 25 mg/L sodium molybdate clearly lower sulphide production in the
387 sediment, and pushed the higher H₂S concentration zone towards deeper sediment layers. Since
388 the transfer of H₂S from sediment to bulk liquid was delayed by this action, molybdate treated
389 samples had lower concentrations of H₂S in the bulk liquid on day 35 when peak concentrations
390 were observed. The H₂S concentration in the bulk liquid did fluctuate in function of time for all
391 treatments, which can be linked to the fact that the set-up used was an open system being
392 continuously exposed to the air inflow and disturbances created during the movement of
393 beakers for microelectrode measurements. The re-introduction of oxygen into the bulk liquid,
394 as confirmed by dissolved oxygen measurements, most likely re-oxidised a portion of the H₂S.
395 In addition, these external disturbances and the nature of the open system might have
396 accelerated H₂S to diffuse to the air from the bulk liquid. Alternatively, H₂S accumulated in the
397 bulk liquid might have reacted with ferrous iron to form iron sulphide that subsequently
398 precipitated in the sediment.

399 The inhibitory concentration of molybdate and a correlation between sulphate and molybdate
400 concentrations were shown in several studies (Biswas et al., 2009; Chen et al., 1998; Jesus et
401 al., 2015). In our previous study, we estimated that the inhibitory concentration for 1500 mg/L
402 sulphate present in our experimental shrimp pond model should be approximately 15 mg/L of
403 sodium molybdate for short-term prevention of H₂S production (Torun et al., 2022). **In the**

404 current study, the molybdate was only partially reduced, both in the M5 and M25 treatments,
405 and the production of H₂S in the sediment and its transfer to bulk liquid could not be fully
406 prevented in the long-term experiment. This might be due to poor diffusion of the molybdate
407 in the deeper layer of the sediment, since in the upper layers of the sediment, there was markedly
408 lower H₂S concentration compared to the control treatment. The reason for molybdate having
409 potentially lower diffusion rates than the sulphate, might be related to adsorption of molybdate
410 on the sediment, as observed for pure quartz sand (Kögler et al., 2021). One can assume that
411 adsorbed molybdate could not inhibit microbial sulphate reduction.

412 In this study, residual sulphate concentrations did not show any apparent difference between
413 the control and molybdate treated samples, but these sulphate concentrations were measured in
414 the bulk liquid. The H₂S and total sulphide productions did show clear differences in the
415 sediment itself, with higher concentrations of sulphide in the control treatment, indicating the
416 effectiveness of molybdate to inhibit sulphate reduction. Residual sulphate in the bulk liquid
417 remained present in all treatments, so despite the high availability of organic matter, sulphate
418 reduction did not continue, as also observed in other studies on shrimp pond sediments (Torun
419 et al., 2022) and other anaerobic ecosystems, such as anaerobic digestion (Lippens and De
420 Vrieze, 2019). This apparent discrepancy was probably due to oxygen intrusion into the water
421 column, halting sulphate reduction in the bulk liquid. Hence, sulphate reduction might have
422 been locally interrupted in the bulk liquid, while it continued in the deeper layers of the
423 sediment.

424 **Overall, it is clear that the biogeochemical sulphur cycle in such a pond system involves**
425 **various processes, i.e., sulphate reduction, sulphide/sulphur (re-)oxidation, precipitation**
426 **of metal sulphides, and production of polysulphides. Due to the nature of the open air**
427 **system (as is the case in real pond systems) in the current study, with the possibility of H₂S**
428 **escaping, it is not possible to make accurate sulphur mass balances.**

429

430 4.2. Molybdate treatment changes the absolute abundance of sulphate reducing bacteria

431 When molybdate is provided in the presence of SRB, ATP sulfurylase uses molybdate (instead
432 of sulphate) and ATP to produce an unstable molecule equivalent to adenosine 5'-
433 phosphosulfate (APS) that cannot be used as electron acceptor (Biswas et al., 2009). Under
434 molybdate excess, some studies indicated that SRB growth could be suppressed altogether.
435 Kögler et al. (2021) showed that there were no SRB specific *dsR* genes isolated when molybdate
436 was continuously injected into sandpacks with residual oil in an oil reservoir. Nair et al. (2015)
437 reported that molybdate concentrations ranging between 50 and 150 μM increased the doubling
438 time of *Desulfovibrio alaskensis* G20, and 500 μM molybdate completely inhibited its cellular
439 growth. In the current study, molybdate was provided only once at lower concentrations than
440 the concentrations mentioned in the literature, but even such lower concentrations of molybdate
441 showed a promising impact towards decreasing sulphide concentrations in the bulk liquid.

442 A higher absolute abundance of the phylum Desulfobacterota, containing several SRB, was
443 detected in molybdate treated samples, despite the fact that mitigation of sulphide production
444 was observed. A similar trend was observed in an earlier study (Tenti et al., 2019), where SRB
445 counts in all samples from a lab-scale anaerobic digester, were similar with or without
446 molybdate, when molybdate concentration was lower than 1.2 mM. In this study, the detection
447 of SRB through 16S rRNA gene amplicon sequencing showed a relative increase of SRB, but
448 did not provide any information on their activity or absolute abundance. Hence, these relative
449 abundances were combined with the absolute cell counts, as obtained through flow cytometry
450 analysis to estimate absolute cell counts of the Desulfobacterota phylum. Such an approach has
451 been successfully applied in other ecosystems, and can be considered an established, reliable
452 way of quantifying microorganisms in environmental samples (Barr et al., 2021; Ou et al., 2017;
453 Props et al., 2017). An overall increasing trend in time was observed for the Desulfobacterota

454 phylum, including the samples treated with molybdate. The reason for the higher absolute
455 abundance of SRB, despite lower H₂S production, might be related to (partial) inactivation of
456 enzymes involved in sulphate reduction. In the study of Nair et al. (2015) on growth and
457 morphology of *Desulfovibrio alaskensis* G20, at least three important enzymes that play a
458 crucial role in energy production (alcohol dehydrogenase, pyruvate carboxylase, tungsten
459 formylmethanofuran dehydrogenase) showed downregulation or repression in the presence of
460 elevated molybdate concentrations. In the current study, molybdate treatment at 25 mg/L
461 showed an overall significantly different bacterial community composition compared to the
462 control without molybdate. The increase in SRB was unexpected, yet, next to sulphate
463 reduction, SRB can also carry out hydrogenic and/or acetogenic metabolisms. Hence, in the
464 absence of sulphate, many SRB can ferment organic acids or alcohol, producing hydrogen
465 acetate or carbon dioxide (Plugge et al., 2011; Zhang et al., 2022). The growth of *Desulfovibrio*
466 on lactate was reported in the absence of sulphate, in syntrophy with a methanogen (Bryant et
467 al., 1977), and the growth of the Delsufovibrionaceae family was also detected in this study.
468 Overall, a combination of reduced H₂S toxicity and the shift in the energy production
469 metabolism appeared to have increased the relative abundance of SRB in this study.
470

471 **5. Conclusions**

472 We showed that molybdate could be an effective mitigation agent against sulphide
473 accumulation in shrimp ponds as a long-term strategy, since it can be applied in a single dose,
474 and at relatively low concentrations. Although, sulphide production could not be avoided
475 completely, **and only a temporal effect could be obtained**, molybdate reduced H₂S production
476 in the sediment, and delayed its transfer to the water column by pushing the sulphide production
477 zone towards deeper sediment layers. Molybdate induced a higher absolute abundance of
478 Desulfobacterota, but this was not reflected in increased sulphide formation. Overall,
479 molybdate ~~can~~ **has the potential to** serve as a more environmentally friendly option compared
480 to other conventional strategies to mitigate sulphide production in shrimp pond systems.

481

482 **Acknowledgments**

483 Special thanks go to the Laboratory of Aquaculture and Artemia Reference Center, Ghent
484 University, for providing shrimp feed (Crevetec Grower 2) and faeces. We would like to thank
485 Koenraad Maréchal and Dirk Raes from Agentschap Natuur & Bos (Belgium) for their help
486 during collection of sediment samples, Tim Lacoere for his assistance with the molecular
487 analyses and Sam Decroo for his assistance with the flow cytometry. The authors also kindly
488 acknowledge Peter Goethals, Peter Bossier, Marleen De Troch and Laurine Burdorf for
489 carefully reading the manuscript.

490

491 **Funding**

492 This research was supported by a Baekeland mandate (Agentschap Innoveren en Ondernemen,
493 VLAIO) through the beneficiary INVE Technologies N.V.

494

495 **Conflict of interest disclosure**

496 The authors declare they have no conflict of interest relating to the content of this article. Jo De
497 Vrieze is a recommender for PCI Microbiology.

498

499 **Data, script, code and supplementary material**

500 The datasets generated and R scripts used during this research are included in this article, its
501 supplementary information, and were submitted to the Zenodo repository
502 (<https://zenodo.org/doi/10.5281/zenodo.10149234>). The raw fastq files that served as a basis
503 for the bacterial community analysis were deposited in the National Center for Biotechnology
504 Information (NCBI) database (Accession number SRP326102).

505

506 **References**

- 507 Avnimelech, Y. and Ritvo, G. 2003. Shrimp and fish pond soils: processes and management.
508 *Aquaculture* 220(1), 549-567.
- 509 Barr, D.A., Omollo, C., Mason, M., Koch, A., Wilkinson, R.J., Lalloo, D.G., Meintjes, G.,
510 Mizrahi, V., Warner, D.F. and Davies, G. 2021. Flow cytometry method for absolute
511 counting and single-cell phenotyping of mycobacteria. *Scientific Reports* 11(1), 18661.
- 512 Baxa, M., Musil, M., Kummel, M., Hanzlík, P., Tesařová, B. and Pechar, L. 2021. Dissolved
513 oxygen deficits in a shallow eutrophic aquatic ecosystem (fishpond) – Sediment oxygen
514 demand and water column respiration alternately drive the oxygen regime. *Science of
515 The Total Environment* 766, 142647.
- 516 Biswas, K.C., Woodards, N.A., Xu, H. and Barton, L.L. 2009. Reduction of molybdate by
517 sulfate-reducing bacteria. *BioMetals* 22(1), 131-139.
- 518 Boon, N., De Windt, W., Verstraete, W. and Top, E.M. 2002. Evaluation of nested PCR-
519 DGGE (denaturing gradient gel electrophoresis) with group-specific 16S rRNA primers
520 for the analysis of bacterial communities from different wastewater treatment plants.
521 *Fems Microbiology Ecology* 39(2), 101-112.
- 522 Boyd, C.E. 1998. Pond water aeration systems. *Aquacultural Engineering* 18(1), 9-40.
- 523 Bryant, M.P., Campbell, L.L., Reddy, C.A. and Crabill, M.R. 1977. Growth of desulfovibrio
524 in lactate or ethanol media low in sulfate in association with H₂-utilizing methanogenic
525 bacteria. *Appl Environ Microbiol* 33(5), 1162-1169.
- 526 Burford, M.A., Peterson, E.L., Baiano, J.C.F. and Preston, N.P. 1998. Bacteria in shrimp pond
527 sediments: their role in mineralizing nutrients and some suggested sampling strategies.
528 *Aquaculture Research* 29(11), 843-849.
- 529 Chen, G., Ford, T.E. and Clayton, C.R. 1998. Interaction of Sulfate-Reducing Bacteria with
530 Molybdenum Dissolved from Sputter-Deposited Molybdenum Thin Films and Pure
531 Molybdenum Powder. *J. Colloid Interface Sci.* 204(2), 237-246.
- 532 Chen, H.-C. 1985 Water quality criteria for farming the grass shrimp, *Penaeus monodon*. Taki,
533 Y., Primavera, J.H. and Llobrera, J.A. (eds), p. 165, Iloilo City, Philippines.
- 534 Dien, L.D., Hiep, L.H., Faggotter, S.J., Chen, C., Sammut, J. and Burford, M.A. 2019. Factors
535 driving low oxygen conditions in integrated rice-shrimp ponds. *Aquaculture* 512,
536 734315.
- 537 Greenberg, A.E., Clesceri, L.S. and Eaton, A.D. (1992) *Standard Methods for the Examination
538 of Water and Wastewater* American Public Health Association Publications,
539 Washington.
- 540 **Huang, C., Luo, Y., Zeng, G., Zhang, P., Peng, R., Jiang, X. and Jiang, M. 2022. Effect
541 of adding microalgae to whiteleg shrimp culture on water quality, shrimp
542 development and yield. *Aquaculture Reports* 22, 100916.**
- 543 Isa, M.H. and Anderson, G.K. 2005. Molybdate inhibition of sulphate reduction in two-phase
544 anaerobic digestion. *Process Biochemistry* 40(6), 2079-2089.
- 545 Jeroschewski, P., Steuckart, C. and Köhl, M. 1996. An Amperometric Microsensor for the
546 Determination of H₂S in Aquatic Environments. *ANALYTICAL CHEMISTRY* 68,
547 4351-4357.
- 548 Jesus, E., Lima, L., Bernardez, L.A. and Almeida, P. 2015. Inhibition of microbial sulfate
549 reduction by molybdate. *Brazilian Journal of Petroleum & Gas* 9, 95.
- 550 Klindworth, A., Pruesse, E., Schweer, T., Peplies, J., Quast, C., Horn, M. and Glockner, F.O.
551 2013. Evaluation of general 16S ribosomal RNA gene PCR primers for classical and
552 next-generation sequencing-based diversity studies. *Nucleic Acids Research* 41(1), 11.
- 553 Kögler, F., Hartmann, F.S.F., Schulze-Makuch, D., Herold, A., Alkan, H. and Dopffel, N.
554 2021. Inhibition of microbial souring with molybdate and its application under reservoir

555 conditions. *Int. Biodeterior. Biodegrad.* 157, 105158.

556 Lippens, C. and De Vrieze, J. 2019. Exploiting the unwanted: Sulphate reduction enables
557 phosphate recovery from energy-rich sludge during anaerobic digestion. *Water*
558 *Research* 163, 114859.

559 Malkin, S.Y., Rao, A.M.F., Seitaj, D., Vasquez-Cardenas, D., Zetsche, E.-M., Hidalgo-
560 Martinez, S., Boschker, H.T.S. and Meysman, F.J.R. 2014. Natural occurrence of
561 microbial sulphur oxidation by long-range electron transport in the seafloor. *Isme j* 8(9),
562 1843-1854.

563 McMurdie, P.J. and Holmes, S. 2014. Waste Not, Want Not: Why Rarefying Microbiome
564 Data Is Inadmissible. *Plos Computational Biology* 10(4), 12.

565 Nair, R.R., Silveira, C.M., Diniz, M.S., Almeida, M.G., Moura, J.J.G. and Rivas, M.G. 2015.
566 Changes in metabolic pathways of *Desulfovibrio alaskensis* G20 cells induced by
567 molybdate excess. *JBIC Journal of Biological Inorganic Chemistry* 20(2), 311-322.

568 Ou, F., McGoverin, C., Swift, S. and Vanholsbeeck, F. 2017. Absolute bacterial cell
569 enumeration using flow cytometry. *J Appl Microbiol* 123(2), 464-477.

570 Panakorn, S. 2016. Hydrogen sulfide- The silent killer. *Aquaculture Asia Pacific Magazine*
571 (March-April), 14-17.

572 Peck, H.D. 1959. THE ATP-DEPENDENT REDUCTION OF SULFATE WITH
573 HYDROGEN IN EXTRACTS OF *DESULFOVIBRIO DESULFURICANS*.
574 *Proceedings of the National Academy of Sciences* 45(5), 701-708.

575 Plugge, C.M., Zhang, W., Scholten, J.C. and Stams, A.J. 2011. Metabolic flexibility of sulfate-
576 reducing bacteria. *Front Microbiol* 2, 81.

577 Props, R., Kerckhof, F.M., Rubbens, P., De Vrieze, J., Hernandez Sanabria, E., Waegeman, W.,
578 Monsieurs, P., Hammes, F. and Boon, N. 2017. Absolute quantification of microbial
579 taxon abundances. *Isme j* 11(2), 584-587.

580 Ranade, D.R., Dighe, A.S., Bhirangi, S.S., Panhalkar, V.S. and Yeole, T.Y. 1999. Evaluation
581 of the use of sodium molybdate to inhibit sulphate reduction during anaerobic digestion
582 of distillery waste. *Bioresour Technol* 68(3), 287-291.

583 Schwermer, C.U., Ferdelman, T.G., Stief, P., Gieseke, A., Rezakhani, N., Van Rijn, J., De Beer,
584 D. and Schramm, A. 2010. Effect of nitrate on sulfur transformations in sulfidogenic
585 sludge of a marine aquaculture biofilter. *FEMS Microbiology Ecology* 72(3), 476-484.

586 Smith, R.L. and Klug, M.J. 1981. Electron Donors Utilized by Sulfate-Reducing Bacteria in
587 Eutrophic Lake Sediments. *Appl Environ Microbiol* 42(1), 116-121.

588 Stoeva, M.K. and Coates, J.D. 2019. Specific inhibitors of respiratory sulfate reduction:
589 towards a mechanistic understanding. *Microbiology (Reading)* 165(3), 254-269.

590 Suo, Y., Li, E., Li, T., Jia, Y., Qin, J.G., Gu, Z. and Chen, L. 2017. Response of gut health and
591 microbiota to sulfide exposure in Pacific white shrimp *Litopenaeus vannamei*. *Fish*
592 *Shellfish Immunol* 63, 87-96.

593 Tenti, P., Roman, S. and Storelli, N. 2019. Molybdate to prevent the formation of sulfide
594 during the process of biogas production. *bioRxiv*, 2019.2012.2012.874164.

595 Thulasi, D., Muralidhar, M. and Saraswathy, R. 2020. Effect of sulphide in Pacific white
596 shrimp *Penaeus vannamei* under varying oxygen and pH levels. *Aquaculture Research*
597 51(6), 2389-2399.

598 Torun, F., Hostins, B., De Schryver, P., Boon, N. and De Vrieze, J. 2022. Molybdate
599 effectively controls sulphide production in a shrimp pond model. *Environmental*
600 *Research* 203, 111797.

601 Torun, F., Hostins, B., Teske, J., De Schryver, P., Boon, N. and De Vrieze, J. 2020. Nitrate
602 amendment to control sulphide accumulation in shrimp ponds. *Aquaculture* 521,
603 735010.

604 Torun, F., Matisli, F., Hostins, B., De Schryver, P., Boon, N. and De Vrieze, J. 2023 Different

605 organic waste loads changes the efficacy of molybdate to control sulphide accumulation
606 in a shrimp pond model, Ghent University, Ghent, Belgium.
607 US-EPA 2011 Hydrogen Sulfide; Community Right-to-Know Toxic Chemical Release
608 Reporting, pp. 64022-64037.
609 Vismann, B. 1996. Sulfide species and total sulfide toxicity in the shrimp Crangon crangon.
610 Journal of Experimental Marine Biology and Ecology 204(1), 141-154.
611 Will, F. and Yoe, J.H. 1953. Colorimetric Determination of Molybdenum with Mercaptoacetic
612 Acid. Analytical Chemistry 25, 1363-1366.
613 Zhang, Z., Zhang, C., Yang, Y., Zhang, Z., Tang, Y., Su, P. and Lin, Z. 2022. A review of
614 sulfate-reducing bacteria: Metabolism, influencing factors and application in
615 wastewater treatment. Journal of Cleaner Production 376, 134109.
616

617 **Tables:**

618 **Table 1** Molybdate concentrations of bulk liquid samples taken from the sacrificed replicates
619 on day 16, 30 and 44. At the end of the experiment (day 61), all three remaining replicates were
620 analysed, hence, the values for day 61 are average values and standard deviations of biological
621 replicates. M5 = Treatment with 5 mg/L molybdate addition. M25 = Treatment with 25 mg/L
622 molybdate addition.

	Molybdate concentration (mg/L)			
	Day 16	Day 30	Day 44	Day 61
Control	0.0	0.0	0.0	0.0 ± 0.0
M5	5.9	4.2	4.5	4.8 ± 4.3
M25	21.9	15.7	12.0	11.6 ± 0.7

623

624 **Table 2** Sulphate concentrations of bulk liquid samples taken from the sacrificed replicates on
625 day 16, 30 and 44. At the end of the experiment (day 61), all three remaining replicates were
626 analysed, hence, the values for day 61 are average values and standard deviations of biological
627 replicates. M5 = Treatment with 5 mg/L molybdate addition. M25 = Treatment with 25 mg/L
628 molybdate addition.

	Sulphate concentration (mg/L)			
	Day 16	Day 30	Day 44	Day 61
Control	1396	1207	1283	1170 ± 206
M5	1334	1201	1261	1021 ± 75
M25	1389	1206	1351	1100 ± 78

629

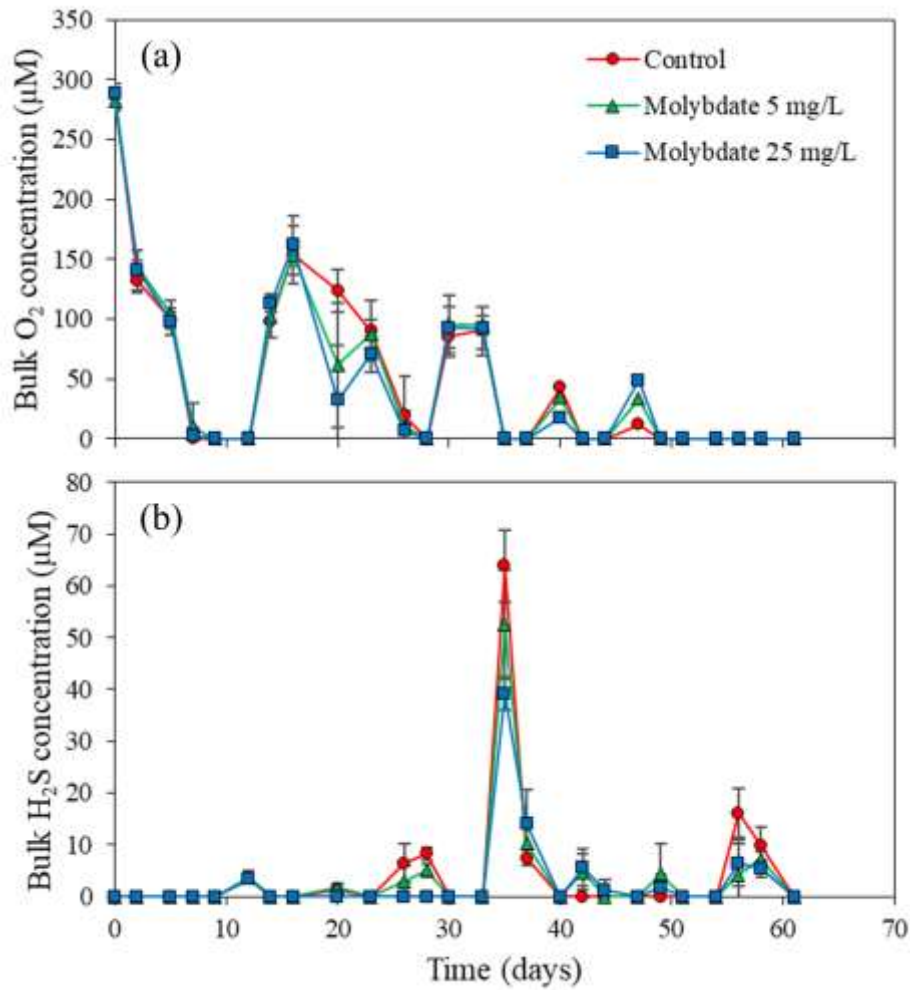
630

631 **Table 3** Absolute cell counts of the Desulfobacterota (10^4 cells per mL), which contains several
632 sulphate reducing bacteria (SRB), as determined by combining flow cytometry cell counts with
633 amplicon sequencing data. The values are average values and standard deviations of biological
634 replicates. M5 = Treatment with 5 mg/L molybdate addition. M25 = Treatment with 25 mg/L
635 molybdate addition.

	Control	M5	M25
Day 16	10.4 ± 1.0	8.3 ± 0.9	19.1 ± 2.3
Day 30	15.2 ± 1.1	12.2 ± 1.9	20.5 ± 4.5
Day 44	21.9 ± 2.5	15.2 ± 0.4	23.7 ± 4.1
Day 61	24.3 ± 6.7	37.3 ± 6.8	29.1 ± 5.3

636

637 **Figures:**



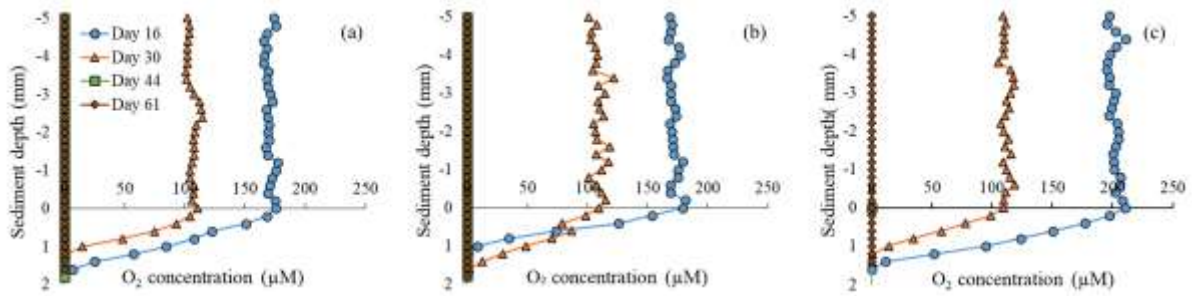
638

639 **Figure 1** The bulk liquid concentrations of (a) O₂ and (b) H₂S in the control treatment,

640 molybdate treatment at 5 mg/L (M5) and molybdate treatment at 25 mg/L (M25). Values

641 represent averages of biological triplicates, and error bars represent the standard deviation.

642



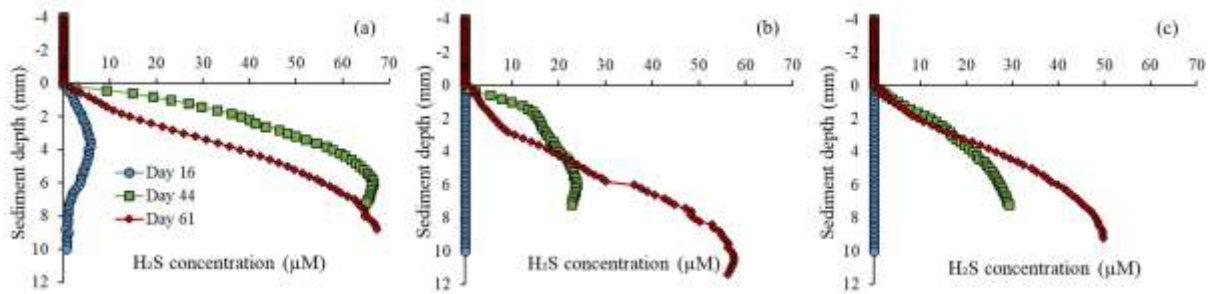
643

644 **Figure 2** The O₂ depth profiles for the (a) control treatment, (b) molybdate treatment at 5 mg/L

645 (M5) and (c) molybdate treatment at 25 mg/L (M25). Values represent averages of biological

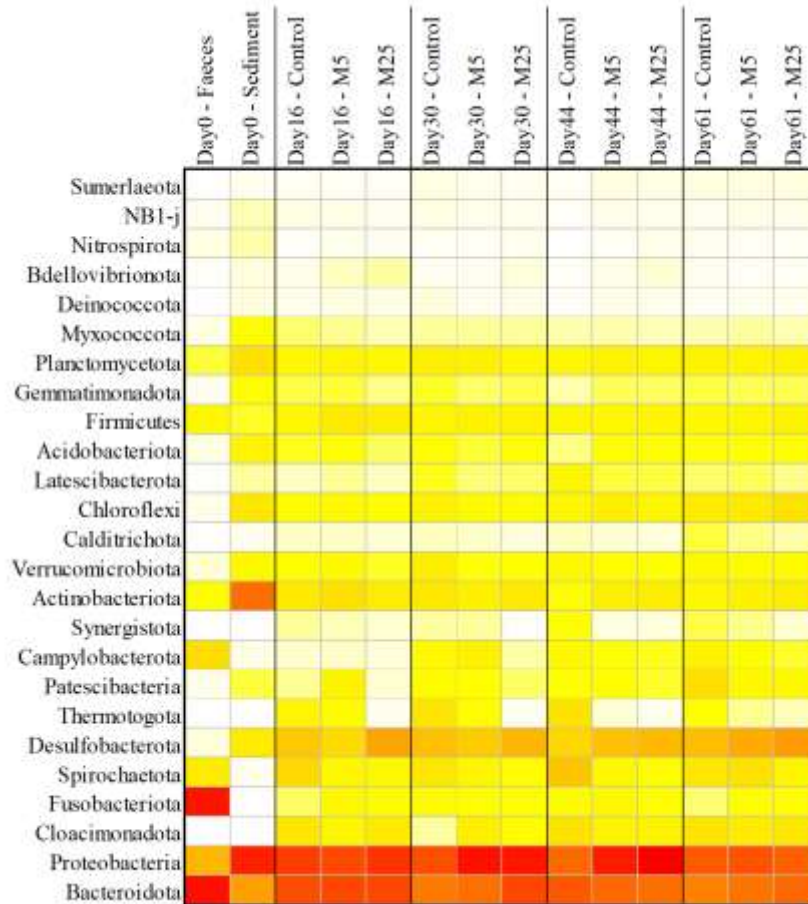
646 triplicates, error bars are omitted to maintain the visibility of the graphs. Zero depth equals to

647 the sediment-water interface. On day 44 and 61, all O₂ values were below the detection limit.



648

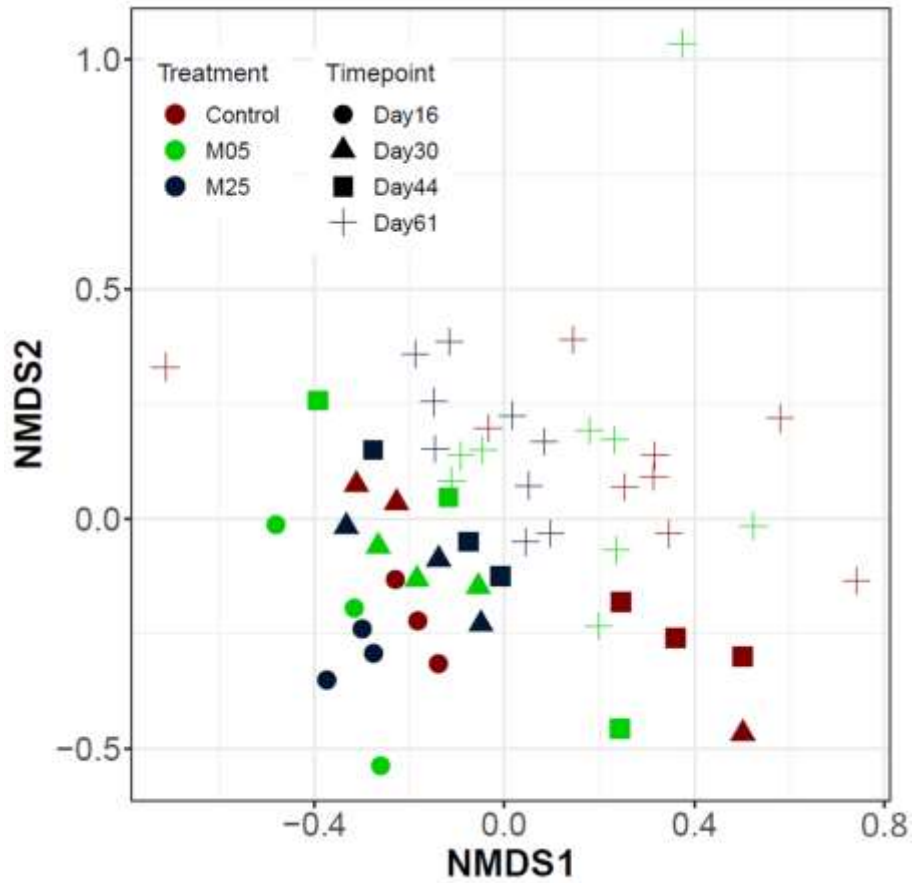
649 **Figure 3** The H₂S depth profiles for the (a) control treatment, (b) molybdate treatment at 5
 650 mg/L (M5) and (c) molybdate treatment at 25 mg/L (M25). Values represent averages of
 651 biological triplicates, error bars are omitted to maintain the visibility of the graphs. Zero depth
 652 equals to the sediment-water interface. Because of technical problems with the microelectrode,
 653 data from day 30 are not included.



654

655 **Figure 4** Heatmap showing the relative abundance of the bacterial community at the phylum
 656 level in the faeces, the sediment and the different treatments on day 16, 30, 44 and 61. Weighted
 657 average values of the biological replicates are presented. The colour scale ranges from 0 (white)
 658 to 40% (red) relative abundance.

659



660

661 **Figure 5** Non-metric multidimensional distance scaling (NMDS) analysis of the Bray-Curtis

662 distance measure of the bacterial community based on amplicon sequencing data at OTU level.

663 Different colours and symbols are used for different treatments and timepoints, respectively.